

BLU-945, a potent and selective next-generation EGFR TKI, has antitumor activity in models of osimertinib-resistant non-small-cell lung cancer

Sun Min Lim , Stefanie S. Schalm, Eun Ji Lee , Sewon Park, Chiara Conti, Yves A. Millet, Rich Woessner, Zhuo Zhang, Luz E. Tavera-Mendoza, Faith Stevison, Faris Albayya, Thomas A. Dineen, John Hsieh, Seung Yeon Oh, Alena Zalutskaya, Julia Rotow, Koichi Goto, Dae-Ho Lee, Mi Ran Yun and Byoung Chul Cho 

Abstract

Introduction: Despite the availability of several epidermal growth factor receptor (EGFR) tyrosine kinase inhibitors (TKIs), most patients with non-small-cell lung cancer (NSCLC) eventually develop resistance to these agents. Notably, *EGFR_C797S* mutations confer resistance to the third-generation EGFR-TKI osimertinib and no approved post-osimertinib targeted pharmacology options are currently available. BLU-945 is a novel, reversible, and orally available next-generation EGFR-TKI that selectively targets EGFR-activating (*EGFRm*) and resistance mutations (including *EGFR_C797S*) with nanomolar potency while sparing wild-type EGFR in vitro.

Methods: In vitro activity of BLU-945 as a single agent and in combination with osimertinib was tested in engineered *EGFR*-mutant cell lines as well as patient-derived cells and patient-derived organoids. In vivo activity was evaluated in osimertinib-resistant patient-derived xenograft mouse models. Three patient cases from the global, first-in-human, phase I/II SYMPHONY trial (NCT04862780) demonstrating the clinical efficacy of BLU-945 were reported.

Results: In vitro BLU-945 demonstrated inhibited cell viability and growth of *EGFR*-mutant/osimertinib-resistant cell lines. BLU-945 demonstrated in vivo tumor shrinkage in osimertinib-resistant models of NSCLC (osimertinib second line: *EGFR_L858R/C797S* and third line: *EGFR_ex19del/T790M/C797S* and *L858R/T790M/C797S*) both as monotherapy and in combination with osimertinib. BLU-945 also demonstrated tumor shrinkage in patients from the SYMPHONY trial.

Conclusion: Our findings demonstrate the preclinical and early clinical activity of BLU-945 in *EGFRm* NSCLC progressing on previous EGFR-TKIs.

Keywords: BLU-945, clinical trial design, drug resistance, EGFR, EGFR inhibitors, NSCLC, osimertinib, patient-derived xenograft, TKI

Received: 15 January 2024; revised manuscript accepted: 19 August 2024.

Introduction

Lung cancer is the second-most common cancer, accounting for over 2.2 million new global cancer diagnoses and approximately 1.8 million deaths worldwide in 2020.^{1,2} Non-small-cell lung cancer

(NSCLC) accounts for 84% of lung cancers in the United States (USA).³ In a subset of NSCLC, specific mutations in the epidermal growth factor receptor (EGFR) gene result in ligand-independent receptor activation leading to uncontrolled

Ther Adv Med Oncol

2024, Vol. 16: 1–20

DOI: 10.1177/
17588359241280689

© The Author(s), 2024.
Article reuse guidelines:
sagepub.com/journals-
permissions

Correspondence to:

Mi Ran Yun
Severance Biomedical
Science Institute, Yonsei
University College of
Medicine, Seoul, Republic
of Korea
fortune@yuhs.ac

Byoung Chul Cho
Division of Medical
Oncology, Department of
Internal Medicine, Yonsei
University College of
Medicine, 50-1 Yonsei-ro,
Seodaemun-gu, Seoul
03722, Republic of Korea
CB1971@yuhs.ac

Sun Min Lim
Division of Medical
Oncology, Department of
Internal Medicine, Yonsei
University College of
Medicine, Seoul, Republic
of Korea

Stefanie S. Schalm
Chiara Conti
Yves A. Millet
Rich Woessner
Zhuo Zhang
Luz E. Tavera-Mendoza
Faith Stevison
Faris Albayya
Thomas A. Dineen
John Hsieh
Alena Zalutskaya
Blueprint Medicines
Corporation, Cambridge,
MA, USA

Eun Ji Lee
Seung Yeon Oh
Department of Biomedical
Science Institute,
Graduated School of
Medical Science, Brain
Korea 21 FOUR Project for
Medical Science, Yonsei
University College of
Medicine, Seoul, Republic
of Korea

Sewon Park
JEUK Institute for Cancer
Research, JEUK Co. Ltd.,
Seoul, Republic of Korea



Julia Rotow

Dana-Farber Cancer
Institute, Boston, MA, USA

Koichi Goto

Department of Thoracic
Oncology, National Cancer
Center Hospital East,
Kashiwa, Japan

Dae-Ho Lee

Department of Oncology,
Asan Medical Center
University of Ulsan College
of Medicine, Seoul,
Republic of Korea

tumor cell survival and proliferation.⁴ The incidence of *EGFR* activating mutations (*EGFRm*) in NSCLC is 10%–40%, and the most common mutations are deletions identified in exon 19 (ex19del) and L858R point mutations in exon 21.⁵ Although patients with NSCLC harboring *EGFRm* benefit from targeted treatment with USA Food and Drug Administration (FDA)-approved *EGFR*-tyrosine kinase inhibitors (TKIs), such as first-generation (1G) gefitinib and erlotinib, second-generation (2G) afatinib and dacomitinib, and third-generation (3G) osimertinib,^{6–10} resistance eventually occurs.^{11,12} The majority of patients on 1G and 2G TKIs develop an *EGFR_T790M* mutation and data suggest *EGFR_C797S* is a common resistance mechanism to the 3G irreversible TKI osimertinib, although resistance often develops due to multiple mechanisms including *KRAS* mutation, *MET* amplification, and loss of *EGFR_T790M* mutation.^{11,13,14}

Osimertinib is an irreversible mutant-selective *EGFR*-TKI, effective in both *EGFRm* TKI-naïve and *EGFRm* patients with NSCLC who developed *EGFR_T790M*-mediated resistance to prior *EGFR* inhibitors.⁹ Unfortunately, despite a higher overall survival with osimertinib treatment (54%; 95% CI, 48–60), compared to gefitinib or erlotinib treatment (44%; 38–50) at 36 months in the first-line setting in patients with locally advanced or metastatic *EGFRm* NSCLC, osimertinib's efficacy is limited by acquired resistance, with progression-free survival (PFS) of 18.9 months.¹⁵ Specifically, in the first-line setting, the median PFS of osimertinib in the *EGFR_L858R* mutant subset was 14.4 months versus 21.4 months in the *EGFR_ex19del* subset.¹⁶ Therefore, *EGFR_L858R* mutations, which represent up to 32% of newly diagnosed *EGFRm* NSCLC,¹⁷ remain an unmet need that osimertinib does not fully address. Furthermore, when patients progress, resistance mechanisms to osimertinib in the first- and second-line settings are comparable.¹¹ Currently, there are no approved targeted pharmacology options post-3G TKI failure.^{11,18} Several preclinical studies indicate that cells harboring *EGFR_T790M-cis/C797S* are resistant to reversible (gefitinib, erlotinib) and covalent (afatinib, dacomitinib, osimertinib) *EGFR*-TKIs, whether used alone or in combination.^{19–21} Therefore, there is an unmet need for TKIs that can effectively target *EGFR_T790M-cis/C797S* and *EGFR_C797S* tumors.

BLU-945 is a next-generation, investigational *EGFR*-TKI developed to inhibit activating and

on-target-resistant *EGFR* mutations, with the potential to prevent disease progression. BLU-945 has on average >450-fold biochemical mutant selectivity over *EGFR* wild type (WT)²² and has shown antitumor activity in nonobese diabetic/severe combined immunodeficiency (NOD/SCID) mice bearing engineered Ba/F3 (*EGFR_ex19del/T790M/C797S* and *EGFR_L858R/T790M/C797S*) tumors.²³

In this study, we evaluated the inhibitory activity of BLU-945 and its effect on *EGFR* phosphorylation as a second-line or third-line treatment option in osimertinib-resistant Ba/F3 cell lines (*EGFR_L858R/C797S*, *EGFR_ex19del/C797S*, *EGFR_ex19del/T790M/C797S*, and *EGFR_L858R/T790M/C797S*) and its antitumor activity in patient-derived models (*EGFR_ex19del/C797S*, *EGFR_L858R/C797S*, and *EGFR_ex19del/T790M/C797S*). In addition, we present initial clinical case reports from the SYMPHONY trial (NCT04862780), an open-label, first-in-human, phase I/II study designed to evaluate the safety, tolerability, and antitumor efficacy of BLU-945 as monotherapy and in combination with osimertinib in patients with *EGFRm* NSCLC.

Materials and methods

Generation of *EGFR*-mutant Ba/F3 cell lines

Cloning of human *EGFR*-mutant coding sequence into p.LVX.IRES.Puro lentiviral vector was performed by Crown Bioscience (San Diego, CA, USA). All cloned colonies were positively confirmed by sequencing. Viral particles were produced by transfecting p.LVX.IRES.Puro vectors into HEK293 cells using Trans-Lentiviral ORF Packaging Kit (GE Healthcare, Chicago, IL, USA). 48 h post-transfection, virus-containing supernatants were harvested and incubated for 48–72 h with parental Ba/F3 cells in the presence of IL-3. Stably transduced Ba/F3 cells were then selected with puromycin (0.5 µg/mL). When confluence was seen, cells were grown in an IL-3-deprived medium to render them solely dependent on transduced *EGFR*-mutant gene activity for survival.

AlphaLISA assay

Mutant *EGFR*-expressing Ba/F3 cells were treated with BLU-945, osimertinib, or gefitinib at 10 different concentrations ranging from 0.095 to 25,000 nM. 0.1% dimethyl sulfoxide (DMSO)

and 25,000 nM staurosporine were used as negative and positive controls, respectively. After 4 h of treatment, cells were processed using the Phospho-EGFR (Tyr1068) AlphaLISA SureFire Ultra Detection Kit (PerkinElmer) according to the manufacturer's instructions. The plate was read on an EnVision multilabel plate reader (PerkinElmer) and the percentage of EGFR phosphorylation inhibition was calculated. Half-maximal inhibitory concentration (IC₅₀) values were calculated using a four-parameter logistic curve.

Generation of PC9_DC cell lines

A PC9_DC cell line containing *EGFR_ex19del/C797S* mutations was constructed using CRISPR technology to introduce *C797S* mutation into PC9 (*EGFR_ex19del*) cells. CRISPR Cas9 plasmid (Cat No. 632601) was purchased from Clontech Laboratories, Inc. (San Jose, CA, USA), and the single-guide RNA and single-strand oligonucleotide template were synthesized from Macrogen (Seoul, Korea).

Establishment of patient-derived preclinical models

Patient-derived cell lines (PDCs; YU-1097 and YU-1182) and patient-derived organoids (PDOs; YUO-143) were established from malignant effusions of patients as previously described.^{24,25} The established PDCs were maintained and passed by general cell culture methods. For PDOs, cells were suspended in cold Matrigel (Corning #256231) and then seeded in 24-well culture plates (Corning, NY, USA). After a 15-min incubation at 37°C, the complete organoid medium (DMEM/F12 medium (Invitrogen, Waltham, MA, USA) supplemented with 20% conditioned R-spondin1 medium, 10 mmol/L HEPES (Invitrogen), 1× GlutaMax (Invitrogen), and 1× antibiotic-antimycotic (Invitrogen)) was added to the solidified Matrigel cells. To determine whether patient-derived preclinical models maintained patient characteristics, Sanger sequencing and whole-exome sequencing were further performed.

Cell viability assay

Cells were seeded and incubated for 3 days for Ba/F3 cells, PC9, PC9_DC, YU-1182, and YU-1097. Viability was measured using CellTiter-Glo[®] assay (Promega, Madison, WI, USA). Organoids were treated with Dispase for 30 min and then pellets

were collected, washed with organoid medium without 20% conditioned R-spondin1 medium, and filtered using a strainer (pluriSelect). Twenty thousand to 70,000 nm organoids were seeded with 5% Matrigel onto 96-well ULA (Ultra-Low Attachment) plates (2×10^3 /well). Cells were incubated with various concentrations of drugs for 5 days. Cell viability was analyzed using Cell Titer Glo-3D (Promega) according to the manufacturer's protocol. Dose-response curves were generated and used to calculate IC₅₀ values using the GraphPad Prism (Ver. 5, GraphPad Software Inc, Boston, MA, USA). All experiments were performed in triplicate and results of biological replicates are presented.

Colony-forming assays

Colony-forming assays were performed by seeding the cells in six-well plates in growth media with appropriate drug-containing media replaced every 3 days. Plates were fixed in 4% PFA and stained in 0.2% crystal violet for 1 h after 14 days of drug treatment.

Antibodies and western blotting

Snap-frozen engineered Ba/F3 cells, YU-1182, YU-1097, and YUO-143 were lysed in RIPA buffer after treatment. Antibodies for phospho-EGFR (Tyr1068; #2234, 1:1000), EGFR (#4267, 1:1000), phospho-alpha serine/threonine-protein kinase (phospho-AKT; Ser473; #9271, 1:1000), AKT (#9272, 1:1000), phospho-ERK1/2 (Thr202/Tyr204; #4370, 1:1000), ERK1/2 (#4696, 1:2000), phospho-S6 kinase (phospho-S6K; #4858; 1:2000), and S6K (#2217; 1:1000) were purchased from Cell Signaling Technology (Danvers, MA, USA). Antibody for β-actin (#A3854; 1:10,000) was purchased from Sigma. Individual band intensities were used for quantification.

In vivo studies

Patient-derived xenograft (PDX) models (YHIM-1094) were established as previously described.²⁶ To generate YU-1097 PDC-derived tumor xenograft models, cells (5×10^6 in 100 μL) were implanted subcutaneously into the flanks of 6-week-old female nu/nu mice. To generate an EGFR_L858R/C797S-expressing Ba/F3 syngeneic injection model, cells (3×10^6 in 200 μL) were implanted into the flank of female NOD-SCID mice.

Prior to the onset of drug treatment, mice were measured for tumor size in two dimensions and the tumor volume (mm^3) was calculated using formula $V = 0.5 a \times b^2$ where a and b are the long and short diameters of the tumor in mm, respectively. Mice were randomly grouped when the tumor volume reached 200mm^3 and allocated to the following treatment groups: vehicle, osimertinib (25 mg/kg once daily [QD]), BLU-945 (100 mg/kg twice daily [BID]), and combinations of osimertinib with BLU-945. BLU-945 and osimertinib were formulated in 20% Solutol HS 15 with 0.5% methylcellulose and dosed orally for 30 days.

Tumor size and body weight were measured twice weekly. Tumor growth inhibition (TGI) was calculated with two formulas according to Drilon et al.²⁷:

$$\begin{aligned} \text{If } TV_t > TV_0, \text{ TGI} &= 100 \times \\ &[1 - (TV_t - TV_0) / (CV_t - CV_0)] \\ \text{If } TV_t < TV_0, \text{ TGI} &= 100 \times [2 - (TV_t / TV_0)] \end{aligned}$$

where TV_0 was the tumor volume in the treatment group at the beginning of the study, TV_t was the tumor volume in the treatment group at the end of the study, CV_0 was the tumor volume in the control group at the beginning of the study, and CV_t was the tumor volume in the control group at the end of the study.

Animals were euthanized if the tumor volume exceeded 2000mm^3 or if tumors became ulcerated/necrotic, and tumor samples were harvested and snap-frozen for subsequent analysis.

Sanger sequencing

Genomic DNA was extracted from PDCs and PDOs using the DNeasy Blood & Tissue Kits (Qiagen, Venlo, Netherlands). Sanger sequencing of the *EGFR* gene was performed at Macrogen.

Immunohistochemistry

Immunohistochemistry staining was performed using the following antibodies: phosphorylated EGFR (pEGFR; #182618; Abcam, Cambridge, UK) and Ki67 (#9027, Cell Signaling Technology).

Statistical analysis

Statistical testing was performed using GraphPad Prism 5. A p -value of < 0.05 was considered statistically significant.

Clinical study

SYMPHONY (NCT04862780) was a phase I/II open-label, international, multicenter dose-escalation and expansion trial of BLU-945 as a single agent or in combination with osimertinib in adults with *EGFRm* metastatic NSCLC. The primary objectives of the dose-escalation part were to assess safety and tolerability and to identify the maximum tolerated dose and/or recommended phase II dose of BLU-945, and BLU-945 in combination with osimertinib. BLU-945 monotherapy and BLU-945 in combination with osimertinib were administered in 28-day cycles. BLU-945 was administered as 25 or 100 mg capsules to be taken either QD or BID on an empty stomach. Osimertinib was administered as 80 mg QD tablets in accordance with the approved product label, local prescribing information, and institutional standards. The SYMPHONY trial was conducted in accordance with written Standard Operating Procedures, in compliance with the Declaration of Helsinki and applicable global/local Good Clinical Practice regulations and International Council for Harmonization guidelines.

Plasma next-generation sequencing (for circulating tumor deoxyribonucleic acid profiling)

Patient cycle 1 day 1 (baseline) and cycle 1 day 15 (on-treatment) whole blood specimens were collected in Streck cell-free DNA blood collection tubes. Using an established protocol generated and executed by Foundation Medicine Inc. (FMI; Cambridge, MA, USA), tubes were gently mixed by inversion and double-centrifuged to separate the plasma from the buffy coat and red blood cells. Circulating tumor deoxyribonucleic acid (ctDNA) was isolated and purified from plasma, followed by library construction and hybrid capture methodologies. Sequencing was performed on the Illumina NovaSeq platform, sequence data were analyzed, and final variant calls were reported using FMI's proprietary software platform.

Results

Activity of BLU-945 as a single agent in EGFR mutant Ba/F3 engineered mouse cell lines

BLU-945 is an oral EGFR-TKI that selectively targets EGFR-activating mutations *EGFR*_L858R and *EGFR*_ex19del, *EGFRm*_T790M, and *EGFRm*_T790M/C797S while sparing

Table 1. Nanomolar inhibition of EGFR mutations by BLU-945 compared to other TKIs.

Compound	Cellular pEGFR inhibition IC ₅₀ (nM)			
	Engineered Ba/F3 cell lines			
	ex19del/C797S	L858R/C797S	ex19del/T790M/C797S	L858R/T790M/C797S
BLU-945	108.8	28.9	4.4	2.9
Gefitinib	6.7	4.4	4864.7	6707.7
Osimertinib	8294.4	7012.0	>10,000	7754.6

EGFR, epidermal growth factor receptor; ex19del, exon 19 deletion; IC₅₀, half-maximal inhibitory concentration; pEGFR, phosphorylated EGFR; TKIs, tyrosine kinase inhibitors.

EGFR-WT.²³ BLU-945 does not interact with the C797S residue of the mutated EGFR and it is approximately fivefold more potent against *EGFR_L858R* compared to *EGFR_ex19del* mutation based on biochemical assays. Details of the discovery and chemical structure of BLU-945 have been previously described by Eno *et al.*²³

The pEGFR inhibitory activity of BLU-945 was evaluated in a series of engineered Ba/F3 cell lines expressing the most common first- and second-line on-target *EGFR*-resistant mutations (*EGFR_ex19del/C797S*, *EGFR_L858R/C797S*, *EGFR_ex19del/T790M/C797S*, and *EGFR_L858R/T790M/C797S*) utilizing a phosphorylation-specific EGFR AlphaLISA assay. In *EGFR_ex19del/C797S* and *EGFR_L858R/C797S* cells, BLU-945 displayed potent inhibition of EGFR phosphorylation with IC₅₀ values of 108.8 and 28.9 nM versus 8294.4 and 7012.0 nM for osimertinib, whereas gefitinib displayed IC₅₀ values of 6.7 and 4.4 nM, respectively (Table 1 and Figure 1(a) and (b)). Consistent with the biochemical IC₅₀ values observed in the AlphaLISA assay performed in this study and that from the study conducted by Eno *et al.*,²³ BLU-945 displayed stronger activity on *EGFR_L858R/C797S* than *EGFR_ex19del/C797S* mutations. In addition, BLU-945 displayed potent inhibition of pEGFR in Ba/F3 cells harboring *EGFR_ex19del/T790M/C797S* and *EGFR_L858R/T790M/C797S* mutations, with IC₅₀ values of 4.4 and 2.9 nM compared to > 10,000 and 7754.6 nM for osimertinib and 4864.7 and 6707.7 nM for gefitinib (Figure 1(c) and (d)). Western blots confirmed BLU-945 selectively and potently inhibits pEGFR and downstream signaling molecules including pAKT, pERK, and pS6K when compared to osimertinib in Ba/F3 cell lines harboring *EGFR_ex19del/T790M/C797S* (Figure 1(e))

and *EGFR_L858R/T790M/C797S* (Figure 1(f)). Cell viability assays were performed to observe the effects of BLU-945 compared to osimertinib on cell growth. BLU-945 demonstrated nanomolar antiproliferative potency with IC₅₀ values of 15 and 6 nM in Ba/F3 cells harboring *EGFR_ex19del/T790M/C797S* and *EGFR_L858R/T790M/C797S*, respectively, compared to > 1000 nM for osimertinib (Figure 1(g) and (h)). Furthermore, in engineered Ba/F3 cells harboring *EGFR_ex19del*, *EGFR_L858R*, *EGFR_ex19del/T790M*, and *EGFR_L858R/T790M* mutations, BLU-945 showed potent anti-proliferative effects comparable to osimertinib (Supplemental Figure 1). BLU-945 specifically demonstrated anti-proliferative effects in *EGFRm* which was not observed in *EGFR-WT* Ba/F3 cells.

Activity of BLU-945 as a single agent and in combination with osimertinib in osimertinib-resistant in vitro cell lines and patient-derived models as a second-line treatment

To assess the activity of BLU-945 as a single agent and in combination with osimertinib in vitro in a second-line setting, cell viability assays, colony formation assays, and western blots were conducted in two osimertinib-resistant *EGFRm* models: YU-1182 and PC9_DC.

Cell viability and western blotting were conducted in the YU-1182 PDC model. This model was derived from a patient with *EGFR_L858R/C797S* NSCLC whose tumor initially expressed the *EGFR_L858R* and developed the *EGFR_C797S* mutation 18 months after first-line treatment with osimertinib (Figure 2(a)). In this model, BLU-945 displayed an IC₅₀ value of 293 nM which is lower than osimertinib (>1000 nM; Figure 2(b)). The immunoblot blot

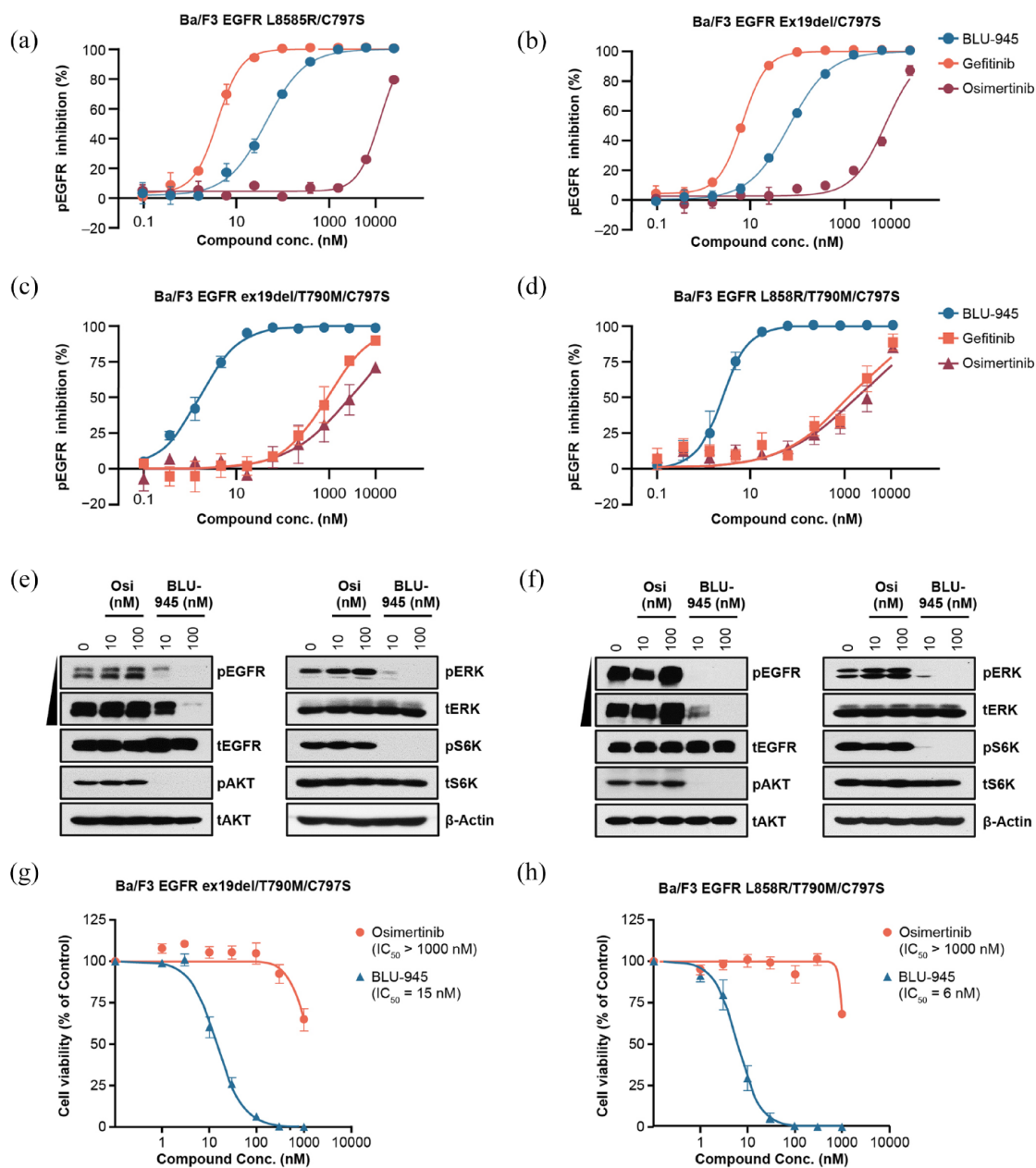


Figure 1. In vitro inhibitory activity of BLU-945 as a second-line or third-line treatment in Ba/F3 cell lines with EGFR mutations. [a–d] Inhibition of pEGFR levels in engineered Ba/F3 cells expressing (a) EGFR_ex19del/C797S mutations, (b) EGFR_L858R/C797S mutations, (c) EGFR_ex19del/T790M/C797S mutations, and (d) EGFR_L858R/T790M/C797S mutations; all treated with BLU-945, gefitinib, and osimertinib. pEGFR levels were plotted relative to the vehicle-treated group (vehicle = 100%). Data plotted as mean \pm SEM. [e, f] Western blot analysis of EGFR activity and downstream signaling molecules in Ba/F3 cell lysates expressing (e) EGFR_ex19del/T790M/C797S mutations and (f) EGFR_L858R/T790M/C797S mutations respectively; cells were treated with vehicle or with 10 or 100 nM of osimertinib or BLU-945, respectively. Two bands are shown for pEGFR; the upper band has a short exposure while the lower band has a long exposure. [g, h] Cell viability at 72 h post-treatment with increasing concentrations of osimertinib or BLU-945, in Ba/F3 cells expressing (g) EGFR_ex19del/T790M/C797S mutations and (h) EGFR_L858R/T790M/C797S mutations. IC_{50} values of BLU-945 were 15 and 6 nM, respectively, and IC_{50} values of osimertinib were >1000 nM in both cell lines. Cell viability is plotted as mean \pm SEM relative to the control-treated group (representing 100%). AKT, alpha serine/threonine-protein kinase; EGFR, epidermal growth factor receptor; ERK, extracellular-signal-regulated kinase; ex19del, exon 19 deletion; IC_{50} , half-maximal inhibitory concentration; osi, osimertinib; pEGFR, phosphorylated EGFR; S6K, S6 kinase; SEM, standard error of the mean; tEGFR, total EGFR.

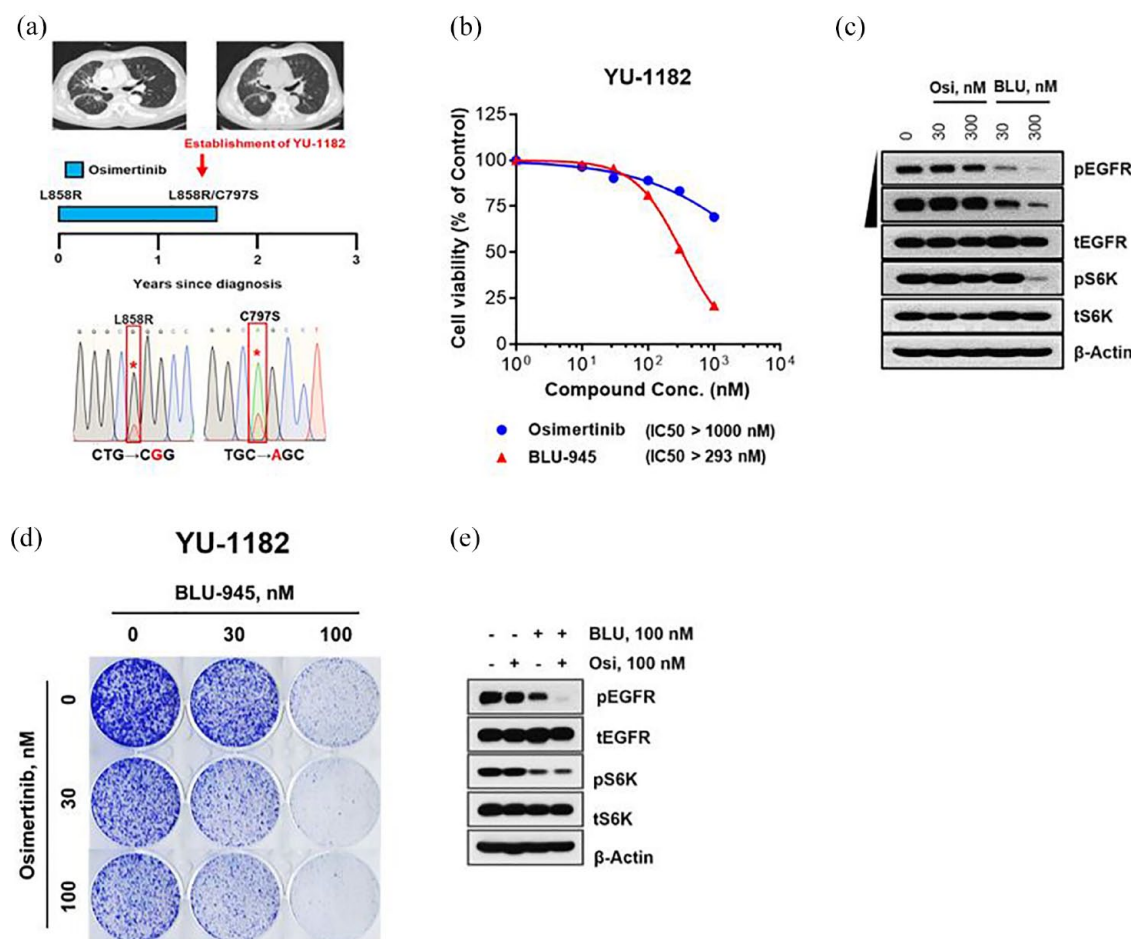


Figure 2. In vitro activity of BLU-945 as a second-line treatment in patient-derived preclinical models and cell lines with C797S mutation. (a) Establishment of a patient-derived cell line (YU-1182) from a patient with *EGFR*-mutant NSCLC who received prior osimertinib, harboring *EGFR*_L858R/C797S. The representative CT images (mediastinal window) display the status of lung cancer at the time of progression on osimertinib. Sanger sequencing performed in this patient shows the development of C797S mutation after first-line osimertinib. The patient therefore developed *EGFR*_L858R/C797S (establishment of YU-1182). (b) Cell viability at 72 h post-treatment with increasing concentrations of osimertinib or BLU-945 in YU-1182. YU-1182 showed resistance to osimertinib (IC₅₀ > 1000 nM) but was sensitive to BLU-945 with an IC₅₀ of 293 nM. Cell viability is plotted as mean ± SEM relative to the control-treated group (representing 100%). (c) Western blot analysis of EGFR activity and downstream signaling molecules in YU-1182 PDC lysates treated with osimertinib and BLU-945 (30 and 300 nM). (d) Colony formation assay investigating the dose-dependent effect of BLU-945 (10, 30, or 100 nM) and osimertinib (30 or 100 nM), either as single agents or in combination on YU-1182 cell survival. DMSO was used as a control. (e) Western blot analysis showing the dose-dependent effect on EGFR activity and downstream signaling molecules in YU-1182 cells following the administration of vehicle, BLU-945 (100 nM), or osimertinib (100 nM), either as single agents or in combination. AKT, alpha serine/threonine-protein kinase; BLU, BLU-945; CT, computerized tomography; DMSO, dimethyl sulfoxide; EGFR, epidermal growth factor receptor; ERK, extracellular-signal-regulated kinase; IC₅₀, half-maximal inhibitory concentration; NSCLC, non-small-cell lung cancer; osi, osimertinib; p, phosphorylated; PDC, patient-derived cell line; S6K, S6 kinase; SEM, standard error of the mean; t, total.

analysis confirmed the inhibition of pEGFR and its downstream signaling molecules by BLU-945 (Figure 2(c)).

When combined, BLU-945 and osimertinib resulted in a dose-dependent inhibition of the

colony formation ability in the YU-1182 model, with the strongest inhibition displayed at the highest drug concentration of 100 nM (Figure 2(d)). Western blot analyses confirmed selective and potent inhibition of pEGFR and downstream signaling molecules in the YU-1182 PDC model

when treated with BLU-945 in combination with osimertinib at 100 nM each (Figure 2(e)). The inhibition was more profound with the combination of BLU-945 and osimertinib when compared to single agents, indicating a combination benefit.

In the cell viability assays conducted in the PC9 and PC9_DC cells, osimertinib demonstrated low nanomolar potency with IC₅₀ values of 10 nM in PC9 cells while displaying weak potency in PC9_DC cells (IC₅₀ values >1000 nM). By contrast, BLU-945 demonstrated similar potency in both the PC9 and PC9_DC cell lines with IC₅₀ values of 408 and 501 nM, respectively (Supplemental Figure 2A). Western blot analyses confirmed selective and potent inhibition of pEGFR and downstream signaling molecules in the PC9_DC cell line when treated with BLU-945 as a single agent at 30 and 300 nM. Osimertinib, however, failed to inhibit the EGFR downstream signaling molecules (Supplemental Figure 2B). Comparable with results observed in the YU-1182 PDC model, a combination (BLU-945 and osimertinib) benefit was demonstrated in the PC9_DC cell line (Supplemental Figure 2C–D).

The antitumor activity of BLU-945 against the C797S mutation was investigated in vivo in a Ba/F3 cell line tumor model harboring *EGFR*_L858R/C797S mutations. Mice were treated with vehicle, osimertinib 25 mg/kg QD, or BLU-945 100 mg/kg BID. Following treatment initiation with BLU-945 100 mg/kg BID, a profound inhibition of tumor growth was observed, which was maintained for up to 40 days. Conversely, vehicle- and osimertinib-treated mice developed progressive disease (Supplemental Figure 3). Collectively, these data demonstrate that BLU-945 is a potent inhibitor of *EGFR*_C797S mutations.

Antitumor activity of BLU-945 as a single agent and in combination with osimertinib as a third-line treatment in patient-derived tumor models harboring EGFR_ex19del/T790M/C797S in vitro

The antitumor activity of BLU-945 as a single agent in the third-line setting was also evaluated in a PDO model (YUO-143) and a PDC model (YU-1097) via a cell viability assay and a western blot. The YUO-143 model was generated from a patient with *EGFR*_ex19del/T790M/C797S NSCLC who had been treated sequentially with

gefitinib, dacomitinib, and osimertinib. The tumor from this patient initially harbored the ex19del mutation and they were treated with gefitinib but further progressed to develop an *EGFR*_T790M mutation 11 months following first-line gefitinib treatment; the patient was subsequently treated with dacomitinib and osimertinib, which resulted in the acquisition of an *EGFR*_C797S mutation. Whole exome sequencing of the patient's tumor showed that the ex19del (mutant allele frequency (MAF), 0.649), T790M (MAF, 0.552), and C797S (MAF, 0.546) mutations existed in a cis-allelic configuration (Figure 3(a) and Supplemental Table 1). BLU-945 produced the strongest anti-proliferative effect with an IC₅₀ value of 40 nM in YUO-143 cells, while osimertinib displayed an IC₅₀ value of >1000 nM (Figure 3(b)). Western blot analysis showed that BLU-945 potently inhibited pEGFR and its downstream signaling molecules (Figure 3(c)).

The second PDC model (YU-1097) was generated from a patient with *EGFR*_ex19del/T790M/C797S NSCLC who had been treated with gefitinib followed by osimertinib. This patient's tumor harbored an *EGFR*_ex19del mutation and was initially treated with gefitinib but then further progressed to develop *EGFR*_T790M 10 months following first-line gefitinib treatment; the patient was subsequently treated with osimertinib, which resulted in the acquisition of an *EGFR*_C797S mutation. Whole exome sequencing of the patient's tumor showed the ex19del (MAF, 0.615), T790M (MAF, 0.382), and C797S (MAF, 0.281) existed in a cis-allelic configuration (Figure 3(d) and Supplemental Table 1). Similar to what was observed in YUO-143 cells, BLU-945 displayed an antiproliferative IC₅₀ value of 108 nM compared to >1000 nM with osimertinib in YU-1097 cells indicating BLU-945's potency (Figure 3(e)). Western blot analysis showed that BLU-945 potently inhibited pEGFR and its downstream signaling molecules (Figure 3(f)).

The antitumor activity of BLU-945 in combination with osimertinib was assessed in a colony formation assay conducted in the YU-1097 PDC model. This model expressing *EGFR*_ex19del/T790M/C797S mutations displayed a dose-dependent decrease in colony-forming ability, with the greatest inhibition in cell survival observed with the combination of BLU-945 and osimertinib (100 nM each; Figure 3(g)). Immunoblot analyses also confirmed the

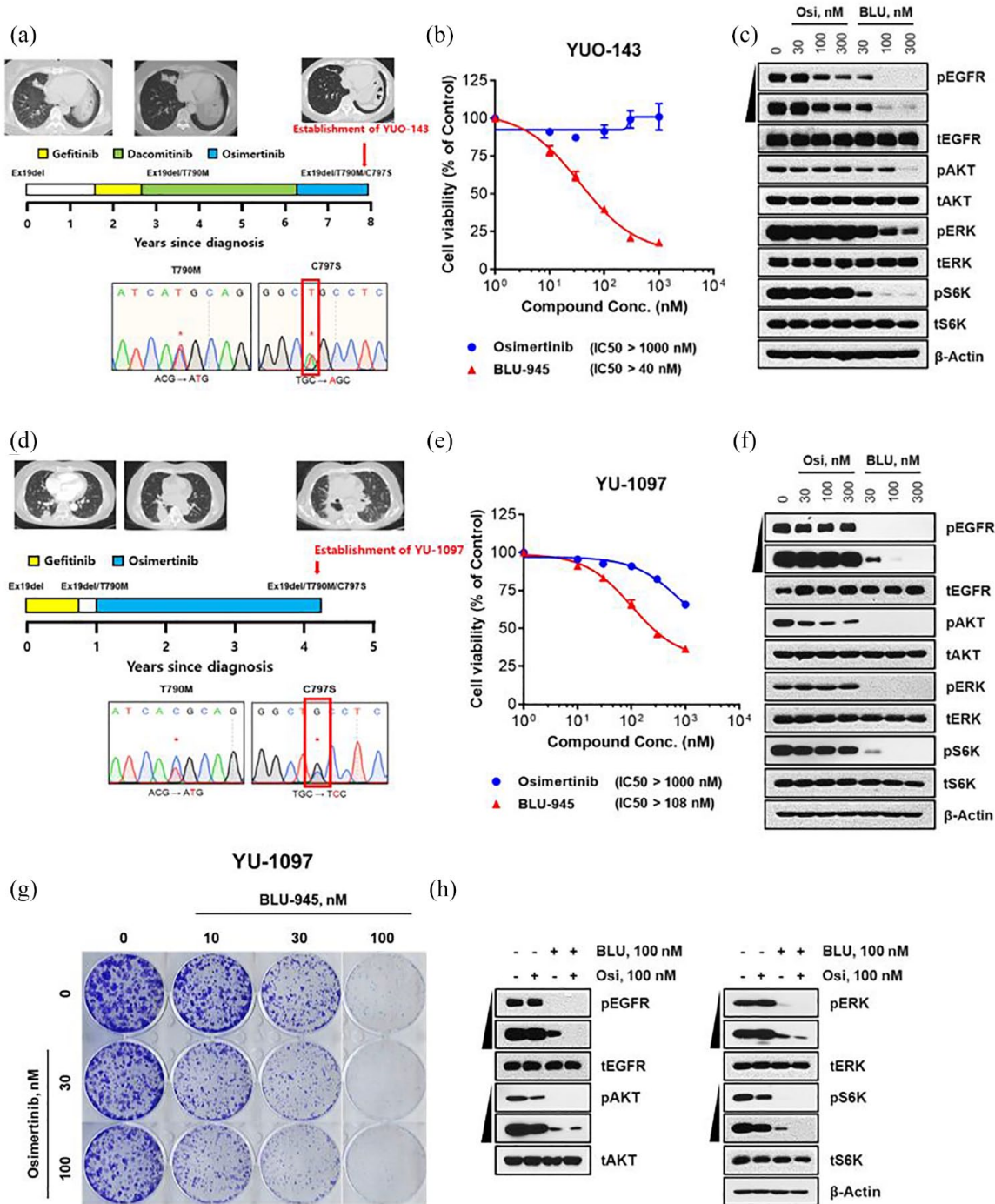


Figure 3. In vitro activity of BLU-945 as a single agent and in combination with osimertinib as a third-line treatment in osimertinib-resistant patient-derived models. (a) Establishment of a PDO (YUO-143) from a patient with *EGFR*-mutant NSCLC who received prior gefitinib, dacomitinib, and osimertinib, harboring *EGFR*_{ex19del/T790M/C797S} mutation. The representative CT images (mediastinal window) display the status of the lung cancer at the time of progression to respective TKI (gefitinib, dacomitinib, and osimertinib). Sanger sequencing performed in this patient showed development of T790M mutation after first-line gefitinib, and subsequent development of C797S mutation after 21 months with osimertinib. The patient therefore developed *EGFR*_{ex19del/T790M/C797S} (establishment of YUO-143). (b) Cell viability at 120 h post-treatment with increasing concentrations of osimertinib or BLU-945 in YUO-143. YUO-143 showed resistance to osimertinib

(Continued)

Figure 3. (Continued)

but was sensitive to BLU-945. Cell viability is plotted as mean \pm SEM relative to the control treated group (representing 100%). (c) Western blot analysis of EGFR activity and downstream signaling molecules in YUO-143 cells treated with osimertinib and BLU-945. (d) Establishment of a PDC (YU-1097) from a patient with *EGFR*-mutant NSCLC who received prior gefitinib and osimertinib, harboring *EGFR*_ex19del/T790M/C797S. The representative CT images (mediastinal window) display the status of lung cancer at the time of progression to respective TKI (gefitinib and osimertinib). Sanger sequencing performed in this patient shows the development of T790M mutation after first-line gefitinib, and subsequent development of C797S mutation after osimertinib treatment. The patient, therefore, developed *EGFR*_ex19del/T790M/C797S (establishment of YU-1097). (e) Cell viability at 72 h post-treatment with increasing concentrations of osimertinib or BLU-945 in YU-1097. YU-1097 showed resistance to osimertinib ($IC_{50} > 1000$ nM) but was sensitive to BLU-945 with an IC_{50} of 108 nM. Cell viability is plotted as mean \pm SEM relative to the control-treated group (representing 100%). (f) Western blot analysis of EGFR activity and downstream signaling molecules in YU-1097 PDC lysates treated with osimertinib and BLU-945. (g) Colony formation assay investigating the dose-dependent effect of BLU-945 (10, 30, or 100 nM) and osimertinib (30 or 100 nM), either as single agents or in combination on YU-1097 cell survival. DMSO was used as a control. (h) Western blot analysis showing the dose-dependent effect on EGFR activity and downstream signaling molecules in YU-1097 cells following the administration of vehicle, BLU-945 (100 nM), or osimertinib (100 nM), either as single agents or in combination.

AKT, alpha serine/threonine-protein kinase; BLU, BLU-945; CT, computerized tomography; DMSO, dimethyl sulfoxide; EGFR, epidermal growth factor receptor; ERK, extracellular-signal-regulated kinase, ex19del, exon 19 deletion; IC_{50} , half-maximal inhibitory concentration; NSCLC, non-small-cell lung cancer; osi, osimertinib; p, phosphorylated; PDC, patient-derived cell line; PDO, patient-derived organoid; S6K, S6 kinase; SEM, standard error of the mean; t, total; TKI, tyrosine kinase inhibitor.

inhibition of EGFR phosphorylation and downstream signaling molecules by BLU-945 combination with osimertinib (Figure 3(h)).

Antitumor activity of BLU-945 in an EGFR_ex19del/T790M/C797S patient-derived xenograft mouse model in vivo

In vivo activity of BLU-945 was assessed in a PDX mouse model (YHIM-1094) derived from the implantation of a tumor from a patient with *EGFR*_ex19del/T790M/C797S NSCLC into a male (NOD-SCID) mouse. This patient was initially treated with gefitinib for an *EGFR*_ex19del mutation and further progressed to develop T790M 12 months following first-line gefitinib treatment; the patient was subsequently treated with osimertinib but later acquired an *EGFR*_C797S mutation (Figure 4(a)). Whole exome sequencing of the patient's tumor showed the ex19del (MAF, 0.78), T790M (MAF, 0.573), and C797S (MAF, 0.402) mutations existed in a cis-allelic configuration (Supplemental Table 1). Once the average tumor volume reached approximately 200 mm³, treatment with vehicle, osimertinib 25 mg/kg QD, or BLU-945 100 mg/kg BID was administered. Vehicle-treated and osimertinib-treated mice developed progressive disease, whereas mice treated with BLU-945 100 mg/kg BID demonstrated substantial tumor regression (Figure 4(b)). No significant differences were observed in the body weight of the

mice between the different treatments (Figure 4(c)). pEGFR and Ki67 (a proliferation marker) levels were analyzed by immunohistochemical staining in tumors derived from YHIM-1094 in the PDX model. We found the number of Ki67-positive tumor cells was significantly lower in the BLU-945-treated group than in the osimertinib-treated or vehicle-treated groups, suggesting anti-proliferative activity in samples treated with BLU-945. Similarly, the intensity of the staining of pEGFR in the osimertinib-treated or BLU-945-treated groups was much weaker than in the vehicle-treated cells (Figure 4(d)), suggesting downregulation of EGFR signaling in samples treated with BLU-945 and osimertinib.

Antitumor activity of BLU-945 in combination with osimertinib in EGFR_ex19del/T790M/C797S osimertinib-resistant models in vivo

In vivo antitumor activity of BLU-945 in combination with osimertinib was assessed in a PDX tumor model established from a PDC (YU-1097). YU-1097 harbored *EGFR*_ex19del/T790M/C797S mutations. Once the average tumor volume reached approximately 200 mm³, treatment with vehicle, osimertinib 25 mg/kg QD, BLU-945 100 mg/kg BID, or a combination of osimertinib 25 mg/kg QD and BLU-945 100 mg/kg BID was initiated. Vehicle-treated and osimertinib-treated mice developed progressive disease, whereas administration of BLU-945 100 mg/kg

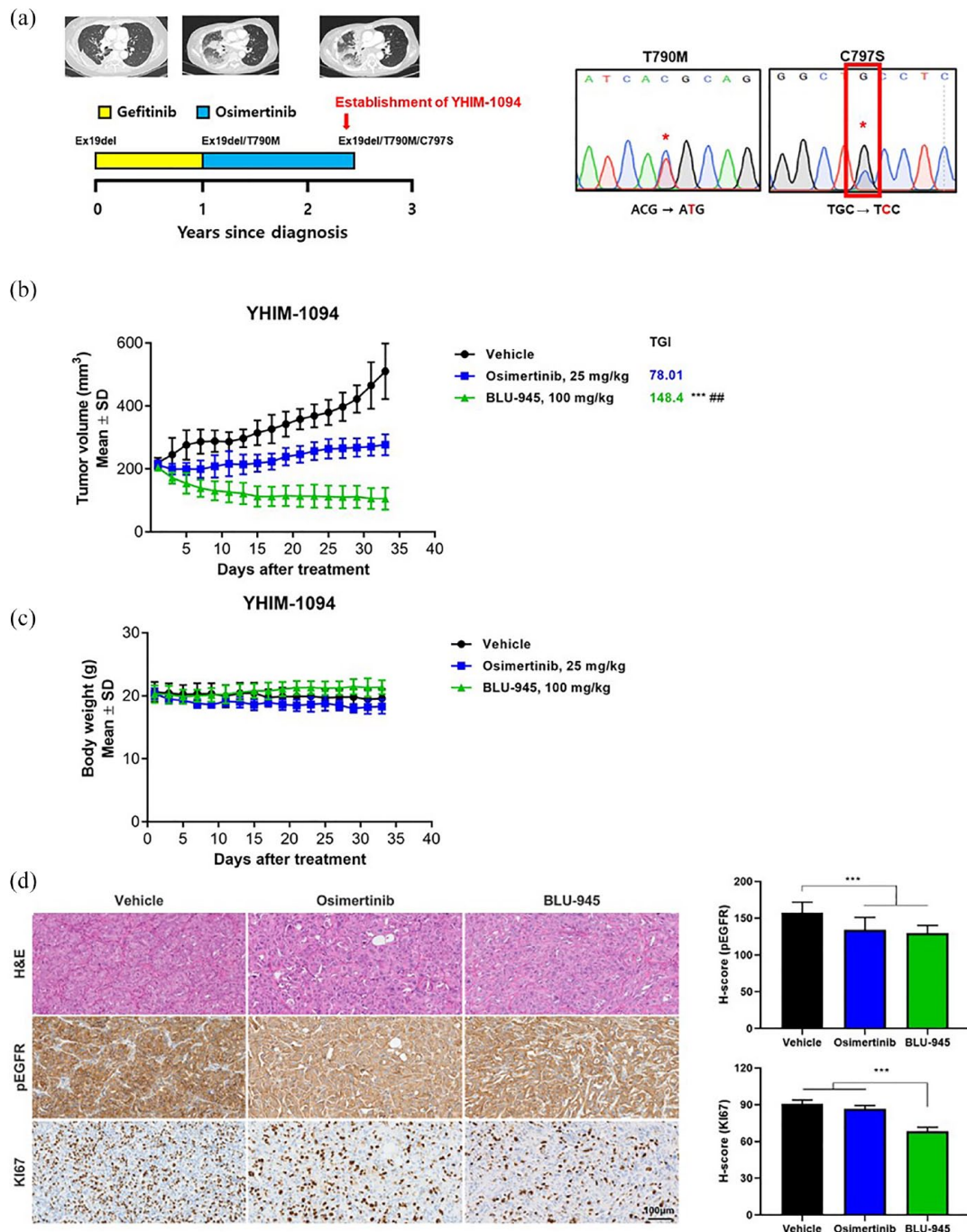


Figure 4. In vivo antitumor activity of BLU-945 as a single agent in the YHIM-1094 osimertinib-resistant *EGFR_ex19del/T790M/C797S* patient-derived xenograft mouse model. (a) Chest CT scans (mediastinal window) of a patient with NSCLC captured after being treated with gefitinib and osimertinib. Sanger sequencing was performed and the presence of the *EGFR_C797S* mutation was detected 16 months following treatment with osimertinib. The patient, therefore, developed the *EGFR_ex19del/T790M/C797S* mutation (establishment of YHIM-1094). Significant difference from vehicle denoted as *** $p < 0.0001$. Significant difference from osimertinib 25 mg/kg denoted as ## $P = 0.002$. (b, c) In vivo antitumor effects of compound BLU-945 in YHIM-1094 patient-derived tumor xenograft. Effects of vehicle (black line), osimertinib at 25 mg/kg (blue line), and BLU-945 at 100 mg/kg (red line) on the growth of YHIM-1094 patient-derived tumor xenograft models for 33 days. (b) Tumor volume during the administration period. (c) Body weight of mice. (d) pEGFR and Ki67 expression in the YHIM-1094 xenografted patient tumor analyzed by IHC. Staining xenografted YHIM-1094 patient tumor treated with vehicle, osimertinib, and BLU-945 (scale bar = 100 μ m). H&E staining was also performed. $N = 6$ animals/group. Data plotted as mean \pm SEM.

CT, computerized tomography; EGFR, epidermal growth factor receptor; ex19del, exon 19 deletion; H&E, hematoxylin and eosin; IHC, immunohistochemistry; NSCLC, non-small cell lung cancer; osi, osimertinib; p, phosphorylated; SEM, standard error of the mean.

BID induced substantial tumor regression (Figure 5(a)). Greater tumor regression was observed with the combination of BLU-945 100 mg/kg BID and osimertinib 25 mg/kg QD. In 6 of 12 mice, there was a body weight loss of more than 10% in the combination treatment group; however, overall there was no significant difference in body weight in mice between the different treatments (Figure 5(b)). We found the number of Ki67-positive tumor cells was significantly lower in the BLU-945-treated group and in the combined BLU-945 and osimertinib-treated group than in the osimertinib-treated or vehicle-treated groups. Similarly, we noticed a lower staining intensity for pEGFR in the BLU-945-treated group and the combined BLU-945 and osimertinib-treated group in comparison to the osimertinib-treated or vehicle-treated groups (Figure 5(c)), indicating a downregulation of EGFR activity.

First-in-human clinical activity of BLU-945 alone and in combination with osimertinib

The antitumor activity of BLU-945 was also assessed in a clinical setting (single agent and in combination with osimertinib). A first-in-human phase I/II clinical trial of BLU-945 (SYMPHONY, NCT04862780) was initiated in April 2021 to assess the safety, tolerability, and efficacy of single agent BLU-945 and in combination with osimertinib in patients with metastatic *EGFR* NSCLC. Three single cases of patients treated in this trial are described here to illustrate the early clinical antitumor activity of BLU-945 as monotherapy and in combination with osimertinib, in heavily pretreated patients harboring *EGFR*_ex19del and T790M ± C797S resistance mutations (Figure 6 and Supplemental Figure 4). In addition, baseline (cycle 1 day 1) and on-treatment (cycle 1 day 15) blood specimens were collected for ctDNA profiling of *EGFR* mutants alleles targeted by BLU-945 for each patient described below.

Case 1. A 53-year-old female with metastatic *EGFR* NSCLC (adenocarcinoma) with *EGFR*_ex19del/C797S mutations detected by local next-generation sequencing (NGS)-based molecular testing which also identified a *CTNNB1* alteration and *NFKB1A*, *NKX2-1*, and *NOTCH3* amplifications at screening. The patient had previously received only osimertinib monotherapy in a metastatic setting. Upon progression on osimertinib, she was enrolled into the BLU-945 in combination with osimertinib (phase I) portion of the

SYMPHONY study without a wash-out period. The patient received a dose of 200 mg BID of BLU-945 and 80 mg QD of osimertinib, continuously in 28-day cycles. Disease assessment after one cycle of treatment showed a partial response (PR) per RECIST v1.1,²⁸ with a -39% change in the sum of the longest diameter of the target compared with baseline. The response was confirmed on the subsequent imaging at 9 weeks of treatment and the sum of the measurements continued to decrease with a -54% change from baseline. The patient maintained their PR up to week 17 before progressing and discontinuing treatment. Marked ctDNA reduction of the ex19del mutant allele (ex19del E746_A750del) was observed in this case at cycle 1 day 15 of treatment (Figure 6(b)).

Case 2. A 57-year-old male with metastatic *EGFR* NSCLC (adenocarcinoma) and *EGFR*_ex19del/T790M/C797S mutations detected by local NGS-based molecular testing. No additional mutations were detected. The patient had previously received afatinib, osimertinib, and carboplatin in combination with pemetrexed. He was enrolled in the BLU-945 monotherapy phase I dose-escalation portion of the SYMPHONY study at a dose of 400 mg QD, given continuously in 28-day cycles. Disease assessment after one cycle of treatment showed a PR per RECIST v1.1,²⁸ with a -30% change in the sum of the longest diameter of target lesions compared with baseline (Supplemental Figure 4). The PR was confirmed on subsequent scans, and the patient continued treatment for more than 33 weeks. The cycle 1 day 15 results indicated ctDNA reduction of the on-target resistance T790M and C797S mutant alleles (Figure 6(c)).

Case 3. A 68-year-old female with metastatic *EGFR* NSCLC (adenocarcinoma) and *EGFR*_ex19del/T790M/C797S mutations detected by local NGS-based molecular testing at screening which also identified *EGFR*_K754E and TP53 mutations. The patient had previously received cisplatin in combination with vinorelbine, followed by erlotinib and osimertinib. She was enrolled in the BLU-945 monotherapy phase I dose-escalation portion of the SYMPHONY study at a dose of 300 mg BID given continuously in 28-day cycles. However, due to an adverse event (Grade 3 increased aspartate aminotransferase), the dosage of BLU-945 was reduced to 200 mg BID at cycle 5. Disease assessment after one cycle of treatment showed stable disease, followed by a PR at 9 weeks per RECIST v1.1,²⁸

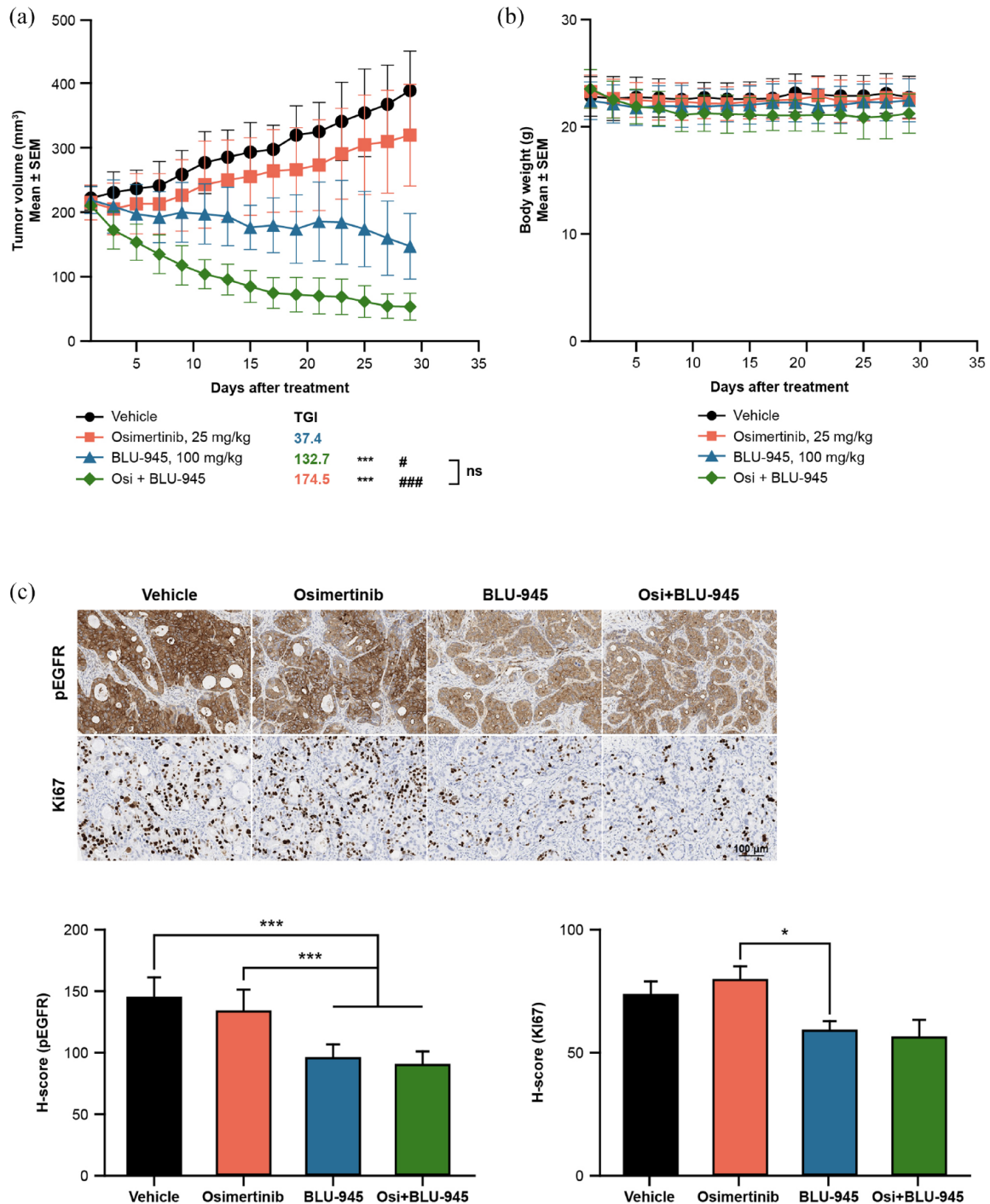


Figure 5. In vivo activity of BLU-945 in combination with osimertinib in patient-derived preclinical models with *EGFR_ex19del/T790M/C797S*. In vivo antitumor effects of compound BLU-945 in YU-1097 patient-derived tumor xenograft mouse model expressing *EGFR_ex19del/T790M/C797S*. Effects of activity of vehicle (black line), osimertinib at 25mg/kg QD (blue line), BLU-945 at 100mg/kg BID (green line), and combination of BLU-945 at 100mg/kg BID and osimertinib at 25 mg/kg QD (red line) in YU-1097 PDX. (a) Tumor volume during the administration period. (b) Body weight of mice. $N=12$ animals/group. Data plotted as mean \pm SEM for all available data at the indicated time point (days), with significance from vehicle marked as ***, $p < 0.001$ and significance from osimertinib 25 mg/kg marked as ## $p = 0.002$ and ### $p < 0.001$. (c) pEGFR and Ki67 expression in the YU-1097 xenografted patient tumor analyzed by IHC. Xenografted YU-1097 patient tumor was treated with vehicle, osimertinib, and BLU-945 (scale bar = 100 μ m). H&E staining was also performed. Data plotted as mean \pm SEM with significance marked as *** $p < 0.001$ and * $p < 0.05$. EGFR, epidermal growth factor receptor; ex19del, exon 19 deletion; H&E, hematoxylin and eosin; IHC, immunohistochemistry; ns, non-significant; osi, osimertinib; p, phosphorylated; PDC, patient-derived cell line; PDX, patient-derived xenograft; SEM, standard error of the mean; TGI, tumor growth inhibition.

with a -38% change in the sum of the longest diameter of target lesions compared with baseline (Figure 6(a)). The PR was confirmed on subsequent scans and continued until progressive disease occurred at 41 weeks. However, this patient continued to derive clinical benefit and remained on treatment post-progression. Cycle 1 day 15 results indicated ctDNA reduction of ex19del (L747_E749del) and K745E as well as reduction of T790M and clearance of C797S on-target resistant resistance mutant alleles (Figure 6(d)).

Discussion

The development of acquired resistance is a major hurdle to successfully treating patients with *EGFR*m NSCLC in the long term, despite the availability of 1G, 2G, and 3G *EGFR*-TKIs. Common *EGFR* mutations in NSCLC include the ex19del mutation, the exon 21 L858R point mutation, and the exon 20 T790M resistance mutation.^{5,29} The most prevalent on-target second-site resistance mutation following a T790M-targeted *EGFR* inhibitor is the C797S mutation.^{23,30} This mutation has been observed in patients following treatment with the 3G *EGFR*-TKI osimertinib, both in the first-line and in the salvage second-line treatment setting.¹¹ There is currently no standard of care nor approved targeted pharmacology options for patients who develop *EGFR*_T790M and C797S mutations. Standard of care varies depending on country but, typically, chemotherapy with or without immunotherapy and vascular endothelial growth factor (VEGF) inhibitors are employed after TKI failure.³¹ However, these regimens are associated with poor PFS and high toxicity in addition to the logistical challenges associated with intravenous administration.³¹

In recent years, several novel treatment strategies for emergent on-target resistance to osimertinib have been explored (e.g., BBT-176, TQB3804, JBJ-04-125-02) and some have demonstrated preclinical activity.^{18,21,32,33} In addition, there are ongoing clinical studies for strategies to extend the benefit of osimertinib treatment. Recently published results from the clinical trial FLAURA2 (NCT04035486) demonstrated osimertinib in combination with chemotherapy improved efficacy including PFS. However, with combination therapy, there were higher rates of grade 3 adverse events and hematologic toxic effects observed versus osimertinib monotherapy and as expected with chemotherapy use.³⁴ BLU-945 is a novel

investigational *EGFR*-TKI capable of inhibiting *EGFR* activating and resistance mutations, notably C797S, which is the most frequently detected on-target resistance mechanism to 3G *EGFR*-TKIs.²³ Antitumor activity of BLU-945 was observed both as a single agent and in combination with osimertinib in osimertinib-resistant preclinical models and in patient cases.

In this paper, we demonstrate both in vitro inhibitory activity and in vivo antitumor activity of BLU-945 (single agent) using engineered Ba/F3 cells, PDC, PDO, and PDX models. In vitro, BLU-945 demonstrated greater inhibition of *EGFR* phosphorylation in cells lines harboring *EGFR*_ex19del/C797S, *EGFR*_L858R/C797S, *EGFR*_ex19del/T790M/C797S, and *EGFR*_L858R/T790M/C797S mutations, compared to osimertinib and gefitinib. While gefitinib is potent against *EGFR*m in NSCLC, *EGFR*_T790M confers resistance to gefitinib³⁵; meanwhile, binding of osimertinib to *EGFR* is inhibited by the C797S mutation.¹¹ The potent inhibition of *EGFR* phosphorylation demonstrated by BLU-945 in the *EGFR* mutated cell lines was confirmed via western blots, which showed downregulation of *EGFR* signaling, and decreased expression levels of the p*EGFR* and downstream signaling molecules. In addition, BLU-945 displayed more potent cellular activity in Ba/F3 cells harboring the *EGFR*_ex19del/T790M/C797S and *EGFR*_L858R/T790M/C797S than osimertinib or gefitinib, for which IC₅₀ values were much higher. BLU-945 showed stronger inhibition of *EGFR* phosphorylation on *EGFR*_L858R/C797S (28.9nM) than on *EGFR*_ex19del/C797S mutations (108.8nM), which is important since current treatments for NSCLC with *EGFR*m show a selectivity bias for *EGFR*_ex19del over *EGFR*_L858R.¹⁶ Of note, while previous reports have shown BLU-945 to have slightly weaker potency against *EGFR*_L858R when compared to 1G *EGFR*-TKIs (i.e., erlotinib, gefitinib), BLU-945 demonstrated higher selectivity against *EGFR*-WT²² and was associated with less *EGFR*-WT-mediated toxicity in the SYMPHONY trial.³⁶

In vivo findings demonstrated that, in comparison to osimertinib, BLU-945 monotherapy led to significant tumor regression in PDX models with *EGFR*_ex19del/T790M/C797S mutations (up to 30 days post-treatment initiation) with no loss in body weight. BLU-945 treatment also resulted in tumor regression and prolonged responses in an osimertinib-resistant *EGFR*_L858R/C797S Ba/

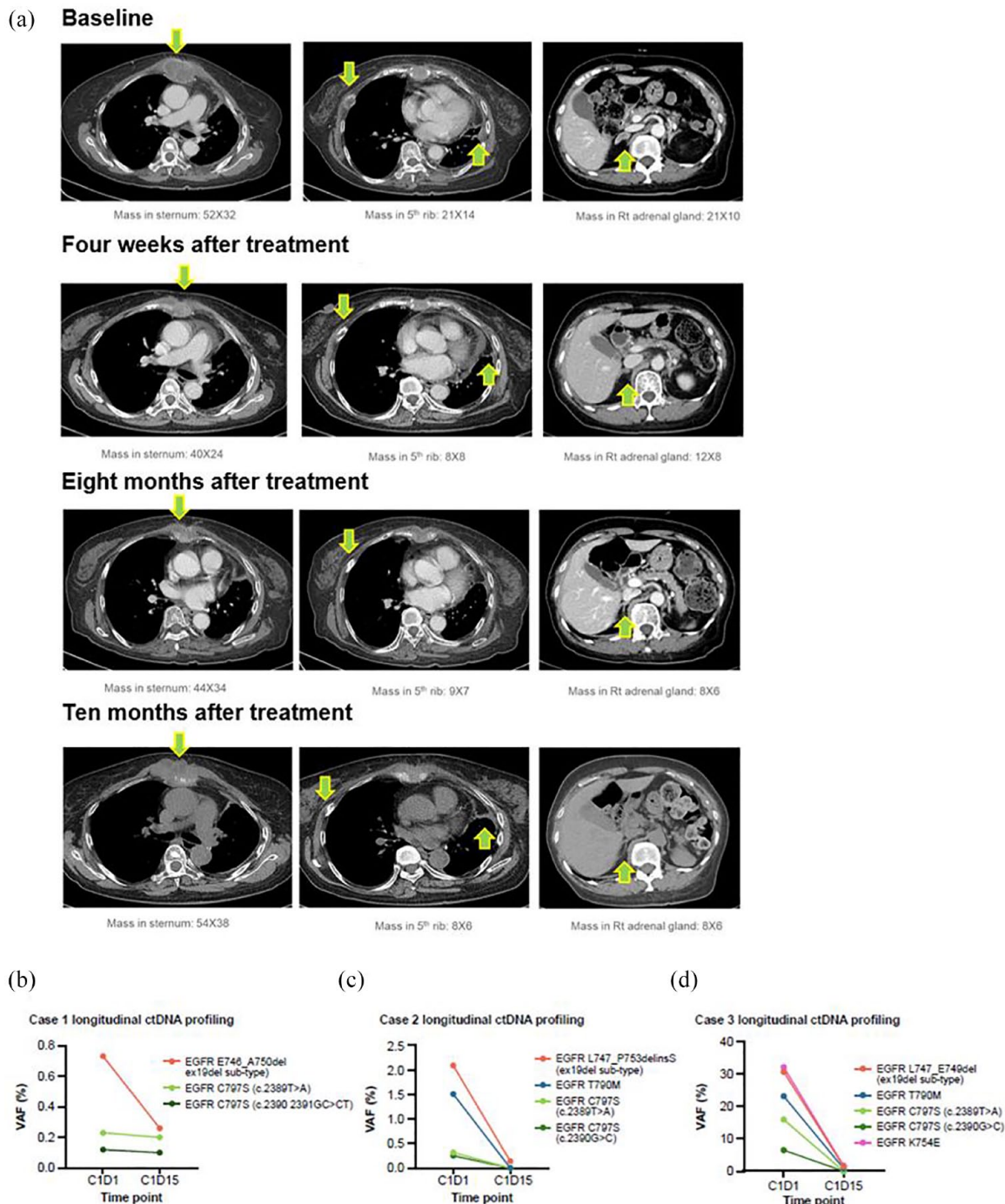


Figure 6. Encouraging early clinical activity with BLU-945. (a) Chest CT scans (mediastinal window) in a 68-year-old woman with advanced adenocarcinoma of the lung harboring *EGFR*_{ex19del/T790M/C797S} (case 3) show marked decrease in the size of mass (arrow) after treatment with BLU-945 monotherapy. Serial CT images were taken at baseline, 4 weeks, 8 months, and 10 months after treatment initiation. Green arrows indicate tumor lesions in the sternum (left panel), fifth rib (middle panel), and adrenal gland (right panel). (b–d) Longitudinal ctDNA profiling via plasma NGS showcasing treatment-induced reductions or clearance of *EGFR*-activating and resistance mutant alleles in three different patients: (b) case 1, (c) case 2, and (d) case 3 at cycle 1 day 15 with detectable *EGFR* mutant allele levels (displayed as VAF (%)) at baseline. CT, computerized tomography; ctDNA, circulating tumor deoxyribonucleic acid DNA; *EGFR*, epidermal growth factor receptor; ex19del, exon 19 deletion; NGS, next-generation sequencing; rt, right; VAF, variant allele frequency.

F3 model in vivo. This is consistent with previous data which showed that BLU-945 was associated with prolonged TGI and survival in a treatment-naïve *EGFR_L858R*-driven preclinical PDX model both as a single agent and in combination with osimertinib versus osimertinib monotherapy.³⁷

In the present study, we also observed inhibition of cell/tumor growth with BLU-945 in combination with osimertinib both in vitro and in vivo. In vitro, BLU-945 with osimertinib inhibited colony formation of cells harboring *EGFR_ex19del/C797S* (PC9_DC) and *EGFR_L858R/C797S* (YU-1182) in a dose-dependent manner. This effect was also observed in a PDO and PDX model expressing *EGFR_ex19del/T790M/C797S* mutations. The enhanced effect may be due to the intracellular allelic heterogeneity.³⁸ In addition, the MAF of the *EGFRm* observed in our preclinical model numerically exceeded that of *EGFR_C797S* and *EGFR_T790M* suggesting a portion of the evolving tumor clone is still driven by the activating mutations that need to be suppressed. Therefore, the combination of osimertinib and BLU-945 could effectively suppress both tumor cells that develop resistance to osimertinib and residual cells driven by the primary *EGFR* mutations in NSCLC.

We have highlighted clinical cases from the SYMPHONY trial showing antitumor activity, including radiologic responses and robust ctDNA reduction or clearance, of BLU-945 in combination with osimertinib post progression (on osimertinib) and as a single agent in heavily pretreated patients with *EGFRm* NSCLC from the phase I dose escalation portion of the SYMPHONY trial. Consistent with preclinical data that demonstrated BLU-945 potency in *EGFR_T790M/C797S* mutants, cases 2 and 3 showed meaningful antitumor activity of BLU-945 monotherapy in heavily pretreated patients with *EGFRm* NSCLC harboring ex19del activating and T790M and C797S resistance mutations. However, because of the recognized tumor heterogeneity due to on-target and off-target treatment resistance following 3G *EGFR*-TKIs,¹¹ combination therapies are viewed as a more promising approach, including in the front-line setting without the presence of resistance. While *EGFR* TKI-TKI combinations have been explored, a high rate of *EGFR*-WT toxicity has limited their clinical utility.³⁹ Case 1

(BLU-945 and osimertinib combination) is particularly interesting as the patient had progressed on osimertinib with the most common on-target *EGFR_C797S* resistance mutation⁴⁰ but later recovered indicating a positive response with the addition of BLU-945, alongside improved tolerance. Osimertinib is the current standard of care in the front-line setting for metastatic *EGFRm* NSCLC, and continuing osimertinib post-progression is a common approach in patients with limited metastatic disease because of the lack of subsequent therapies, which are also often toxic. Therefore, BLU-945 in combination with osimertinib may offer a clinically impactful option to overcome on-target resistance.

A key limitation of our study was the inability to test the antitumor activity of the combination of BLU-945 and osimertinib treatment in *EGFR_L858R/C797S* or *EGFR_ex19del/C797S* mutations in the in vivo models (PDX and Ba/F3 models). The major reasons being, first, it was not possible to identify patients with *EGFR_L858R/C797S* or *EGFR_ex19del/C797S* mutations to establish the PDX models and second, as *EGFR_L858R/C797S* and *EGFR_ex19del/C797S* Ba/F3 models are homogeneous and exclusively driven by *EGFR*, they would have been insensitive to osimertinib (due to the presence of the C797S mutation).

Conclusion

To conclude, these findings suggest BLU-945 may offer meaningful clinical activity in *EGFRm* NSCLC refractory to standard treatments.

Declarations

Author's note

Stefanie S. Schalm is currently affiliated with Enact Bio, Watertown, MA, USA. Rich Woessner is currently an independent consultant. Zhuo Zhang is currently affiliated with BMS, Boston, MA, USA. Luz E. Tavera-Mendoza is currently affiliated with Mariana Oncology, Boston, MA, USA. Faith Stevison is currently affiliated with Constellation Pharmaceuticals, Inc., a fully owned subsidiary of MorphoSys, Inc., Boston, MA, USA. Alena Zalutskaya is currently affiliated with Tyra Biosciences, Boston, MA, USA.

Ethics approval and consent to participate

All animal studies were approved by a local Institutional Animal Care and Use Committee (IACUC) and conducted in accordance with the

regulations of the Association for Assessment and Accreditation of Laboratory Animal Care (AAALAC) and local IACUC guidelines. The SYMPHONY study protocol was approved by the Institutional Review Board of Severance Hospital (IRB No. 4-2016-0001) and all patients provided written informed consent.

Consent for publication

All patients provided written informed consent to publication.

Author contributions

Sun Min Lim: Conceptualization, data curation, investigation, visualization, writing – original draft, writing – review and editing.

Stefanie S. Schalm: Conceptualization, writing – review and editing.

Eun Ji Lee: Data curation, validation, investigation, visualization, methodology, writing – review and editing.

Sewon Park: Data curation, validation, investigation, visualization, writing – review and editing.

Chiara Conti: Conceptualization, data curation, writing – review and editing.

Yves A. Millet: Validation, visualization, writing – original draft, writing – review and editing.

Rich Woessner: Validation, investigation, visualization, writing – review and editing.

Zhuo Zhang: Writing – review and editing.

Luz E. Tavera-Mendoza: Validation, investigation, visualization, writing – review and editing.

Faith Stevison: Conceptualization, validation, investigation, visualization, writing – review and editing.

Faris Albayya: Data curation and writing – review and editing.

Thomas A. Dineen: Validation, visualization, writing – review and editing.

John Hsieh: Validation, investigation, visualization, methodology, writing – review and editing.

Seung Yeon Oh: Data curation, validation, visualization, writing – review and editing.

Alena Zalutskaya: Concept visualization, data curation, writing – review and editing.

Julia Rotow: Validation, investigation, visualization, methodology, writing – review and editing

Koichi Goto: Investigation, methodology, and writing – review and editing.

Dae-Ho Lee: Investigation, and writing – review and editing

Mi Ran Yun: Conceptualization, data curation, formal analysis, supervision, investigation, methodology, writing – original draft, project administration, writing – review and editing.

Byoung Chul Cho: Conceptualization, supervision, methodology, project administration, writing – review and editing.

Acknowledgments

The authors acknowledge the co-investigators on the SYMPHONY trial and thank the patients and their families. Medical writing support was provided by Appitha Eakin, PhD, Paragon, UK, and editorial support was provided by Travis Taylor, BA, Paragon, US, supported by Blueprint Medicines Corporation. Blueprint Medicines Corporation follows all current policies established by the International Committee of Medical Journal Editors and Good Publication Practice guidelines (<https://www.acpjournals.org/doi/epdf/10.7326/M22-1460>). The Sponsor was involved in the study design, collection, analysis, and interpretation of data, as well as data checking of information provided in the manuscript. However, the ultimate responsibility for opinions, conclusions, and data interpretation lies with the authors.

Funding

The authors disclosed receipt of the following financial support for the research, authorship, and/or publication of this article: This research was supported by Blueprint Medicines Corporation.

Competing interests

S.M.L. reports grants from AstraZeneca, BeiGene, Bristol Myers Squibb, Boehringer-Ingelheim, Bridge BioTherapeutics, Daichii-Sankyo, Eli Lilly, Gilead, GlaxoSmithkline, Jiangsu Hengrui Medicine, J Ints Bio, Oscotec, Roche, Takeda, and Yuhan. S.S.S. is a shareholder of Blueprint Medicines Corporation. C.C. is an employee of and a shareholder of Blueprint Medicines Corporation. Y.A.M. is an employee of and a shareholder of Blueprint Medicines Corporation. R.W. is a shareholder of Blueprint Medicines Corporation. Z.Z. is a shareholder of Blueprint Medicines Corporation. L.E.T.-M. reports work was conducted as an employee of Blueprint Medicines Corporation and is currently a shareholder of Blueprint Medicines

Corporation. F.S. is a shareholder of Blueprint Medicines Corporation. F.A. is an employee of and a shareholder of Blueprint Medicines Corporation. T.A.D. is an employee of and a shareholder of Blueprint Medicines Corporation. J.H. is an employee of Blueprint Medicines Corporation and a shareholder of Blueprint Medicines Corporation. A.Z. is a shareholder of Blueprint Medicines Corporation. J.R. reports consulting fees or honoraria from Amgen, AstraZeneca, BioAtla, G1 Therapeutics, Genentech, Guardant Health, Jazz, Janssen, Sanofi-Genzyme, Summit, and Takeda Pharmaceuticals, and has also been contracted for research (institutional) with AstraZeneca, BioAtla, Blueprint Medicines, Enliven, EpimAb Biotherapeutics, LOXO Oncology, ORIC, and Redcloud. D.H.L. reports personal fees from AbbVie, AstraZeneca, BC World Pharm, Boehringer-Ingelheim, Bristol-Myers Squibb, ChongKeunDang, Eli Lilly, Janssen, Merck Sharp & Dohme, Novartis, Ono, Pfizer, Roche, ST Cube, Takeda Oncology, and Yuhan, and non-financial support from Blueprint Medicines Corporation and Takeda Oncology outside the submitted work. B.C.C. reports grants from AbbVie, AstraZeneca, Bayer, Blueprint Medicines Corporation, Champions Oncology, Dizal Pharma, Dong-A ST, Eli Lilly, GI Innovation, Janssen, MedPacto, Merck Sharp & Dohme, MOGAM Institute, Novartis, Ono, Yuhan, and consultancy fees from AstraZeneca, Blueprint Medicines Corporation, Bristol Myers Squibb, Boehringer-Ingelheim, Eli Lilly, Janssen, MedPacto, Merck Sharp & Dohme, Novartis, Ono, Pfizer, Roche, Takeda, and Yuhan and currently owns stock in BridgeBio Therapeutics, Gencurix Inc, KANAPH Therapeutic Inc, TheraCanVac Inc., has served on a scientific advisory board for KANAPH Therapeutic Inc, receives royalties for Champions Oncology and is the founder of Daan Biotherapeutics.

Availability of data and materials

Consistent with expectations of good scientific practice, qualified researchers can request access to data by providing a data request with a commitment to publish their findings. Requests can be submitted via datasharing@blueprintmedicines.com and will be reviewed by the Data Sharing Committee and medical experts, or a relevant publications steering committee.

ORCID iDs

Sun Min Lim  <https://orcid.org/0000-0001-7694-1593>

Eun Ji Lee  <https://orcid.org/0000-0002-4362-939X>

Byoung Chul Cho  <https://orcid.org/0000-0002-5562-270X>

Supplemental material

Supplemental material for this article is available online.

References

1. Sung H, Ferlay J, Siegel RL, et al. Global Cancer Statistics 2020: GLOBOCAN estimates of incidence and mortality worldwide for 36 cancers in 185 countries. *CA Cancer J Clin* 2021; 71(3): 209–249.
2. Zhou C, Wu YL, Chen G, et al. Erlotinib versus chemotherapy as first-line treatment for patients with advanced EGFR mutation-positive non-small-cell lung cancer (OPTIMAL, CTONG-0802): a multicentre, open-label, randomised, phase 3 study. *Lancet Oncol* 2011; 12(8): 735–742.
3. American Cancer Society. Cancer facts & figures, <https://www.cancer.org/content/dam/cancer-org/research/cancer-facts-and-statistics/annual-cancer-facts-and-figures/2019/cancer-facts-and-figures-2019.pdf> (2019, accessed 16 March 2023).
4. Wee P and Wang Z. Epidermal growth factor receptor cell proliferation signaling pathways. *Cancers (Basel)* 2017; 9(5): 52.
5. Hsu WH, Yang JC, Mok TS, et al. Overview of current systemic management of EGFR-mutant NSCLC. *Ann Oncol* 2018; 29(Suppl. 1): i3–i9.
6. Mok TS, Wu Y-L, Ahn M-J, et al. Osimertinib or platinum–pemetrexed in EGFR T790M-positive lung cancer. *N Engl J Med* 2016; 376(7): 629–640.
7. Mok TS, Wu YL, Thongprasert S, et al. Gefitinib or carboplatin–paclitaxel in pulmonary adenocarcinoma. *N Engl J Med* 2009; 361(10): 947–957.
8. Park K, Tan EH, O’Byrne K, et al. Afatinib versus gefitinib as first-line treatment of patients with EGFR mutation-positive non-small-cell lung cancer (LUX-Lung 7): a phase 2B, open-label, randomised controlled trial. *Lancet Oncol* 2016; 17(5): 577–589.
9. Cross DA, Ashton SE, Ghiorghiu S, et al. AZD9291, an irreversible EGFR TKI, overcomes T790M-mediated resistance to EGFR inhibitors

- in lung cancer. *Cancer Discov* 2014; 4(9): 1046–1061.
10. Lavacchi D, Mazzoni F and Giaccone G. Clinical evaluation of dacomitinib for the treatment of metastatic non-small cell lung cancer (NSCLC): current perspectives. *Drug Des Devel Ther* 2019; 13: 3187–3198.
 11. Leonetti A, Sharma S, Minari R, et al. Resistance mechanisms to osimertinib in EGFR-mutated non-small cell lung cancer. *Br J Cancer* 2019; 121(9): 725–737.
 12. Yu HA, Arcila ME, Rekhtman N, et al. Analysis of tumor specimens at the time of acquired resistance to EGFR-TKI therapy in 155 patients with EGFR-mutant lung cancers. *Clin Cancer Res* 2013; 19(8): 2240–2247.
 13. Ramalingam SS, Zhang N, Yu J, et al. MA07.03 real-world landscape of EGFR C797X mutation as a resistance mechanism to osimertinib in non-small cell lung cancer. *J Thorac Oncol* 2022; 17(9 Suppl): S67–S68.
 14. Li Y, Mao T, Wang J, et al. Toward the next generation EGFR inhibitors: an overview of osimertinib resistance mediated by EGFR mutations in non-small cell lung cancer. *Cell Commun Signal* 2023; 21(1): 71.
 15. Ramalingam SS, Vansteenkiste J, Planchard D, et al. Overall survival with osimertinib in untreated, EGFR-mutated advanced NSCLC. *N Engl J Med* 2020; 382(1): 41–50.
 16. Soria JC, Ohe Y, Vansteenkiste J, et al. Osimertinib in untreated EGFR-mutated advanced non-small-cell lung cancer. *N Engl J Med* 2018; 378(2): 113–125.
 17. Riess JW, Gandara DR, Frampton GM, et al. Diverse EGFR exon 20 insertions and co-occurring molecular alterations identified by comprehensive genomic profiling of NSCLC. *J Thorac Oncol* 2018; 13(10): 1560–1568.
 18. Lee J, Piotrowska Z, Soo R, et al. Combatting acquired resistance to osimertinib in EGFR-mutant lung cancer. *Ther Adv Med Oncol* 2022; 14: 17588359221144099.
 19. Rangachari D, To C, Shpilsky JE, et al. EGFR-mutated lung cancers resistant to osimertinib through EGFR C797S respond to first-generation reversible EGFR inhibitors but eventually acquire EGFR T790M/C797S in preclinical models and clinical samples. *J Thorac Oncol* 2019; 14(11): 1995–2002.
 20. Andrews Wright NM and Goss GD. Third-generation epidermal growth factor receptor tyrosine kinase inhibitors for the treatment of non-small cell lung cancer. *Transl Lung Cancer Res* 2019; 8(Suppl 3): S247–S264.
 21. Thress KS, Paweletz CP, Felip E, et al. Acquired EGFR C797S mutation mediates resistance to AZD9291 in non-small cell lung cancer harboring EGFR T790M. *Nat Med* 2015; 21(6): 560–562.
 22. Lim SM, Park C-W, Zhang Z, et al. BLU-945, a fourth-generation, potent and highly selective epidermal growth factor receptor tyrosine kinase inhibitor with intracranial activity, demonstrates robust in vivo anti-tumor activity in models of osimertinib-resistant non-small cell lung cancer. *Presented at AACR Annual Meeting*, 9–14 April 2021; Virtual format.
 23. Eno MS, Brubaker JD, Campbell JE, et al. Discovery of BLU-945, a reversible, potent, and wild-type-sparing next-generation EGFR mutant inhibitor for treatment-resistant non-small-cell lung cancer. *J Med Chem* 2022; 65(14): 9662–9677.
 24. Kim SY, Lee JY, Kim DH, et al. Patient-derived cells to guide targeted therapy for advanced lung adenocarcinoma. *Sci Rep* 2019; 9(1): 19909.
 25. Kim SY, Kim SM, Lim S, et al. Modeling clinical responses to targeted therapies by patient-derived organoids of advanced lung adenocarcinoma. *Clin Cancer Res* 2021; 27(15): 4397–4409.
 26. Kang HN, Choi JW, Shim HS, et al. Establishment of a platform of non-small-cell lung cancer patient-derived xenografts with clinical and genomic annotation. *Lung Cancer* 2018; 124: 168–178.
 27. Drilon A, Ou SI, Cho BC, et al. Repotrectinib (TPX-0005) is a next-generation ROS1/TRK/ALK inhibitor that potently inhibits ROS1/TRK/ALK solvent-front mutations. *Cancer Discov* 2018; 8(10): 1227–1236.
 28. Eisenhauer EA, Therasse P, Bogaerts J, et al. New response evaluation criteria in solid tumours: revised RECIST guideline (version 1.1). *Eur J Cancer* 2009; 45(2): 228–247.
 29. Ma C, Wei S and Song Y. T790M and acquired resistance of EGFR TKI: a literature review of clinical reports. *J Thorac Dis* 2011; 3(1): 10–18.
 30. Wang S, Tsui ST, Liu C, et al. EGFR C797S mutation mediates resistance to third-generation inhibitors in T790M-positive non-small cell lung cancer. *J Hematol Oncol* 2016; 9(1): 59.
 31. Shi C, Wang Y, Xue J, et al. Immunotherapy for EGFR-mutant advanced non-small-cell lung

- cancer: current status, possible mechanisms and application prospects. *Front Immunol* 2022; 13: 940288.
32. Lim SM, Kim D-W, Jung JE, et al. 1365TiP—a phase I/II, open-label study of BBT-176, a triple mutation targeting EGFR TKI, in patients with NSCLC who progressed after prior EGFR TKI therapy. *Presented at ESMO*, 16–21 September 2021; Virtual format.
33. Liu X, Zhang X, Yang L, et al. Abstract 1320: preclinical evaluation of TQB3804, a potent EGFR C797S inhibitor. *Presented at AACR Annual Meeting*, 29 March–April 3 2019, Atlanta, GA.
34. Planchard D, Janne PA, Cheng Y, et al. Osimertinib with or without chemotherapy in EGFR-mutated advanced NSCLC. *N Engl J Med* 2023; 389(21): 1935–1948.
35. Wang Y, Guo Z, Li Y, et al. Development of epidermal growth factor receptor tyrosine kinase inhibitors against EGFR T790M. Mutation in non small-cell lung carcinoma. *Open Med (Wars)* 2016; 11(1): 68–77.
36. Nagasaka M, Shum E, Bazhenova L, et al. BLU-945 monotherapy and in combination with osimertinib (OSI) in previously treated patients with advanced EGFR-mutant (EGFRm) NSCLC in the phase 1/2 SYMPHONY study. *J Clin Oncol* 2023; 41(16 Suppl): 9011.
37. Tavera L, Campbell J, Dhande A, et al. BLU-945 or BLU-701 as single agents versus their combination with osimertinib in EGFR L858R driven tumor models. *Eur J Cancer* 2022; 174: S63.
38. Santoni-Rugiu E, Melchior LC, Urbanska EM, et al. Intrinsic resistance to EGFR-tyrosine kinase inhibitors in EGFR-mutant non-small cell lung cancer: differences and similarities with acquired resistance. *Cancers* 2019; 11(7): 923.
39. Rotow JK, Costa DB, Paweletz CP, et al. Concurrent osimertinib plus gefitinib for first-line treatment of EGFR-mutated non-small cell lung cancer (NSCLC). *J Clin Oncol* 2020; 38: 9507.
40. Fu K, Xie F, Wang F, et al. Therapeutic strategies for EGFR-mutated non-small cell lung cancer patients with osimertinib resistance. *J Hematol Oncol* 2022; 15(1): 173.